
Reinforcing Multimodal Understanding and Generation with Dual Self-rewards

Jixiang Hong¹ Yiran Zhang³ Guanzhong Wang² Yi Liu² Ji-Rong Wen¹ Rui Yan^{1,4*}

¹ GSAI, Renmin University of China

² Baidu Inc.

³ School of Computer Science and Technology, UCAS

⁴ School of Computer Science, Wuhan University

{jxhong, ruiyan}@ruc.edu.cn, zhangyiran232@mails.cas.edu.cn

{wangguanzhong, liuyi22}@baidu.com

Abstract

Building upon large language models (LLMs), recent large multimodal models (LMMs) unify cross-model understanding and generation into a single framework. However, LMMs still struggle to achieve accurate image-text alignment, prone to generating text responses contradicting the visual input or failing to follow the text-to-image prompts. Current solutions require external supervision (e.g., human feedback or reward models) and only address unidirectional tasks—either understanding or generation. In this work, based on the observation that understanding and generation are inverse dual tasks, we introduce a self-supervised dual reward mechanism to reinforce the understanding and generation capabilities of LMMs. Specifically, we sample multiple outputs for a given input in one task domain, then reverse the input-output pairs to compute the dual likelihood of the model as self-rewards for optimization. Extensive experimental results on visual understanding and generation benchmarks demonstrate that our method can effectively enhance the performance of the model without any external supervision, especially achieving remarkable improvements in text-to-image tasks.

1 Introduction

Recently, following the success of LLMs in text-centric tasks, many works have explored extending LLMs to multimodal tasks, leading to the emergence of LMMs. By optionally incorporating modality-specific encoders and decoders (or tokenizers and de-tokenizers), some LMMs are tailored for visual understanding tasks [1, 2], some for visual generation tasks [3], while others are designed to unify both understanding and generation tasks [4–7].

Despite the impressive performance of LMMs in both understanding and generation tasks, they still face challenges in aligning text and image modalities. For visual understanding tasks, LMMs often fail to accurately perceive visual content and return hallucinated or incorrect responses, as illustrated in Figure 1(a). Ji et al. [8], Ouali et al. [9] conduct supervised fine-tuning (SFT) on paired data with preference labels. For text-to-image generation tasks, LMMs tend to generate images that are inconsistent with the text prompts, as shown in Figure 1(b). Jiang et al. [10] propose a two-level chain-of-thought (COT) generation method and employ ensemble rule-based reward models to optimize the model. These efforts often concentrate on improving only one aspect (either understanding or generation) of LMM capabilities, and most of them depend heavily on external supervision signals or parallel text-image pairs data for training.

*Corresponding authors



Figure 1: Failures in visual understanding and image generation of Janus-Pro-7B. In (a), the text in **red** indicates hallucinative content. In (b), the generated images do not follow the content in **orange**.

To address these limitations, we explore how to reinforce the understanding and generation of LMMs in a self-supervised manner, without relying on external supervision and pairing data. We observe that understanding and generation are inherently dual tasks, where the output of one task can naturally serve as the input of the other. Moreover, existing unified LMMs have already undergone basic alignment and demonstrate a certain level of capability in both tasks, but the dual-task relationship is not fully utilized. Motivated by this, we seek to exploit this duality between understanding and generation to enable mutual self-supervision, allowing the optimization of one task to be guided by feedback derived from its dual counterpart. However, to derive self-supervised rewards for both tasks in a unified and efficient way is non-trivial. Existing methods tend to employ visual query-answer (VQA) tasks to assess the generated images in text-to-image (T2I) tasks [11, 12], which is not applicable to understanding tasks. DeGF [13] leverages an auxiliary image generated by Stable Diffusion [14] to improve the understanding performance, which relies on external feedback and is of high cost and latency.

To achieve our objective and tackle the above challenges, we propose a dual self-reward mechanism to provide self supervision for optimizing the understanding and generation of LMMs. Specifically, for visual understanding, we sample multiple textual descriptions given an input image, then reverse the input-output pairs and use each description as the condition to compute the likelihood of generating the original image. This enables a quantitative assessment of how well each description aligns with the visual content. Analogously, for text-to-image generation, we compute the likelihood of generating the original text prompt conditioned on the sampled images to assess their semantic fidelity. By incorporating this dual self-reward mechanism, we can effectively optimize the understanding and generation capabilities in a unified manner. Besides, based on this dual self-reward mechanism, we explore different optimization strategies, including jointly optimizing both capabilities within a single model, as well as alternately optimizing the two capabilities in two adversarial models. We also investigate different optimization methods for this task, including preference optimization and reinforcement learning methods.

Extensive experiments have been conducted on various visual understanding and generation benchmarks to validate the effectiveness of our method. Specifically, we evaluate the performance of our method on the T2I-CompBench [15] and GenEval [16] datasets, which are widely used for assessing the performance of LMMs in text-to-image generation tasks. Our tuned Janus-Pro-7B [7] model gains remarkable improvements over the baseline model, achieving an 11.68% increase on average on T2I-CompBench and a 5% increase on GenEval. Additionally, the model also demonstrates improved performance on visual understanding tasks, for example, achieving a 7.5% increase in the overall score on the LLaVA-Bench².

In summary, our contributions are as follows:

²<https://huggingface.co/datasets/liuhaojian/llava-bench-in-the-wild>

- To the best of our knowledge, we present the first unified self-supervised framework that jointly enhances both the understanding and generation capabilities of large multimodal models (LMMs).
- We propose a dual self-reward mechanism that leverages the inherent duality between understanding and generation tasks to provide self-supervised optimization signals. And we explore different optimization strategies and optimization methods based on the dual self-rewards for unified learning of LMMs.
- We conduct extensive experiments on various visual understanding and generation benchmarks, demonstrating the effectiveness of our method in improving the performance of unified LMMs.

2 Related Work

2.1 Multimodal Understanding and Generation

Visual Understanding. Advancement in large language models (LLMs) has paved the way for the development of large multimodal models (LMMs) for vision-language understanding. These works focus on how to align visual signals with the language semantic space of the pre-trained LLMs. By connecting vision encoders to pre-trained LLMs, LMMs can effectively understand both visual and textual inputs [17, 18]. LLaVA [2] and MiniGPT-4 [19] were among the first to attempt to train adapters to shift the output of the vision encoder into the embedding space of the language model. Qwen-VL [1], InternVL [20] and Deepseek-VL [21, 22] further enhance the visual-linguistic performance on more complex scenarios by incorporating more advanced LLM backbones, additional training data of higher quality and more effective training strategy. Although these models have achieved impressive performance in visual understanding and reasoning, mere perception and comprehension fall short of our broader expectations for multimodal intelligence.

Visual Generation. Recent advances in visual generation can be generally categorized into two main approaches: diffusion models and autoregressive models. The LMMs for visual generation fall in the latter category, which we mainly focus on in this paper. These models typically adopt an autoregressive approach, which is the focus of this paper. These models generate images by producing a sequence of discrete visual tokens, which are then decoded into images using vector-quantized (VQ) model [23, 24] based visual tokenizers. Representative works in this line of research include LlamaGen and DeLVM, which demonstrate the potential of autoregressive modeling in high-fidelity image synthesis within a multimodal framework.

Unified LMM for Understanding and Generation. Unified LMMs aim to integrate both understanding and generation capabilities into a single framework, enabling them to perform a wide range of multimodal tasks. Unified LMMs aim to seamlessly integrate understanding and generation capabilities within a single framework, enabling them to handle a broad spectrum of multimodal tasks. Models like Emu [25], Emu2 [26], X-ViLa [27], and Next-GPT [28] adopt a unified autoregressive architecture that treats both visual embeddings and text tokens as elements to predict. AnyGPT [29], Show-o [5], ViLA-U [30], Chameleon [31], Emu3[4], and Janus series [6, 7], leverage VQ tokenizers to discretize images into tokens, thereby allowing both vision and language to be modeled uniformly through next-token prediction.

2.2 Optimization for Large Multimodal Models

Although the LMMs demonstrated promising performance in various multimodal tasks, they still face challenges in accurately aligning textual and visual modalities. Existing works explore how to conduct fine-grained optimization on LMMs to further improve them. Align-anything [8] propose a framework to align all-modality (any-to-any) models with human intentions using unified language feedback and 200k human preference annotations. SILMM [11] proposes a self-VQA manner and DPO [32] to improve the compositional text-to-image generation performance, while T2I-R1 utilizes ensemble rule-based reward models to reinforce two levels of chain-of-thought (COT) text-to-image generation with GRPO [33]. These methods focus on improving the performance of LMMs in either understanding or generation tasks, and most of them rely on external supervision signals, such as human feedback or reward models, which may not be readily available in all scenarios. Based on the

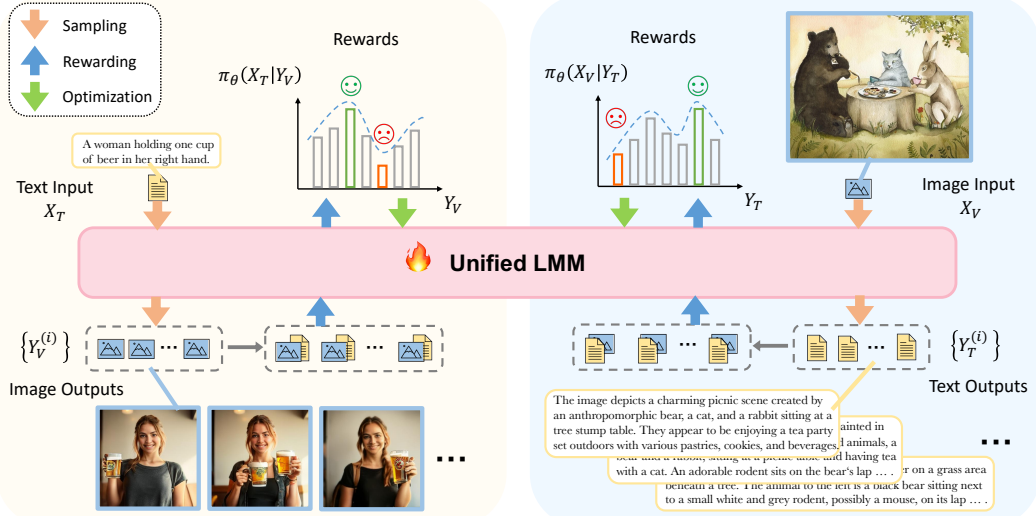


Figure 2: Overview of our dual self-reward mechanism. The model samples multiple outputs for a given input for one task and reverses the input-output pairs to compute the dual likelihoods of the model outputs conditioned on the original input as self-rewards for optimization.

observation that understanding and generation are inherently dual tasks and they can assess the output of each other, we explore a self-supervised dual reward mechanism to reinforce the bi-directional tasks in a unified manner.

3 Methodology

In this section, we first introduce the duality between understanding and generation tasks in unified LMMs. Then we present our dual self-reward mechanism, which leverages the inherent duality between understanding and generation tasks to provide self-supervised optimization signals. Finally, we describe the optimization method used for model optimization based on the self-reward signals. The overview of our dual self-reward mechanism is shown in Figure 2

3.1 Duality between Understanding and Generation

The understanding and generation tasks in unified LMMs are inherently dual tasks. For text-to-image generation, the model takes a text prompt X_T describing the desired content of the image as input and generates an image $Y_V = \{y_v^i\}_{i=1}^{\|Y_V\|}$ that aligns with the text. This process can be formulated as:

$$\pi_\theta(Y_V | X_T) = \prod_{i=1}^{\|Y_V\|} \pi_\theta(y_v^i | X_T, y_v^{<i}), \quad (1)$$

where each vision token y_v^i is generated sequentially based on the previous tokens $y_v^{<i}$ and the text prompt X_T , and π_θ denotes the generation process parameterized by θ . $\|Y_V\|$ is the number of vision tokens in the generated image.

Reversely, for visual understanding, the model takes an image X_V as input and generates a text response $Y_T = \{y_t^i\}_{i=1}^{\|Y_T\|}$ that matches the content of the image. This process can be formulated as:

$$\pi_\theta(Y_T | X_V) = \prod_{i=1}^{\|Y_T\|} \pi_\theta(y_t^i | X_V, y_t^{<i}), \quad (2)$$

where y_t^i denotes the text tokens, and $\|Y_T\|$ is the number of text tokens in the generated response.

These two tasks exhibit natural duality, where the output of one task can serve as the input for the other, especially text-to-image generation and image captioning.

3.2 Dual Self-reward Mechanism

Based on the duality between visual understanding and generation in LMMs, we propose a dual self-reward (DSR) mechanism to provide self-supervised optimization signals for both tasks.

Specifically, for visual understanding, we generate multiple textual descriptions for a given input image; and then reverse the input-output position by treating each generated description as the conditional input and the original image as the target output to compute the likelihood of the image conditioned on each textual description. This procedure is based on the intuitive assumption that: if a textual description accurately reflects the visual input, then the likelihood of generating the original image conditioned on this description should be high. By this, we can effectively quantify how well each description explains and matches the visual content. Similarly, for text-to-image generation, we sample multiple images given a text prompt and compute the likelihood of generating the original text prompt conditioned on each sampled image, which allows us to assess the semantic fidelity of the generated images. We derive the dual self-rewards from the aforementioned reversed likelihoods, which can be expressed as:

$$\begin{aligned} R_U(Y_T | X_V) &= \frac{1}{\|X_V\|} \log \pi_\theta(X_V | Y_T) = \frac{1}{\|X_V\|} \sum_1^{\|X_V\|} \log \pi_\theta(x_v^i | Y_T, x_v^{<i}), \\ R_G(Y_V | X_T) &= \frac{1}{\|X_T\|} \log \pi_\theta(X_T | Y_V) = \frac{1}{\|X_T\|} \sum_1^{\|X_T\|} \log \pi_\theta(x_t^i | Y_V, x_t^{<i}), \end{aligned} \quad (3)$$

where $R_U(Y_T | X_V)$ and $R_G(Y_V | X_T)$ denote the self-rewards for textual response Y_T given visual input X_V in visual understanding task and visual output Y_V given textual prompt X_T in T2I generation tasks, respectively.

Our dual self-reward mechanism naturally possesses the following advantages: 1) efficiency, compared to self-VQA and generating additional reference content, dual self-rewards can be computed in a single forward pass of the model; 2) self-supervised, the dual self-rewards are derived from the model’s own outputs, eliminating the need for external supervision or additional data; 3) unified, the dual self-rewards can be applied to both understanding and generation tasks, allowing for a more comprehensive optimization process; 4) unbiased, the rewards are likelihoods of the same original input for multiple sampled outputs, which can reduce the length bias [34] existing in the reward model based methods [8].

3.3 Optimization with Self-rewards

With the dual self-rewards, we can optimize the model using different optimization methods, including preference optimization and reinforcement learning methods, as well as different optimization strategies.

We adopt the online SimPO [35] method, which is a simple preference optimization method that can be easily applied to LMMs. We also employ the GRPO [33] method, which is a prevalent reinforcement learning method to optimize the reasoning capabilities of LLMs.

Specifically, for each task (visual understanding or generation), we sample G candidate outputs and compute their dual self-rewards. Then we select the highest-reward sample Y^+ and the lowest-reward sample Y^- , and train the model with a pairwise preference objective that encourages the model to prefer the better output. The SimPO objective is defined as:

$$\begin{aligned} \mathcal{J}_{\text{SimPO}}(\theta) &= \mathbb{E}_{X \sim \mathcal{D}, (Y^+, Y^-) \sim \pi_\theta(\cdot | X)} \\ &\left[\log \sigma \left(\frac{\beta}{\|Y^+\|} \log \pi_\theta(Y^+ | X) - \frac{\beta}{\|Y^-\|} \log \pi_\theta(Y^- | X) - \gamma \right) \right], \end{aligned} \quad (4)$$

where β is a scaling factor for the preference margin, and γ is a reward margin used to enforce a separation between the better and worse outputs. where $R(\cdot | \cdot)$ denotes the corresponding dual self-reward from Section 3.2, and $\sigma(\cdot)$ is the sigmoid function. This objective encourages the model to assign a higher likelihood to outputs that better align with the input according to the DSR.

We also employ the GRPO [33] method, which estimates the advantage in a group-relative manner without relying on a value function, making it suitable for optimizing LMMs with self-reward signals.

Following DAPO [36], we adopt a higher clipping threshold and a token-level policy gradient loss in the GRPO objective.

Given an input X (either X_T for generation or X_V for understanding), the model samples a group of G outputs $\{Y^{(i)}\}_{i=1}^G$ under the reference policy $\pi_{\theta_{\text{ref}}}$, each associated with a dual self-reward $R^{(i)} = R(Y^{(i)} | X)$ as defined in Section 3.2.

The group-normalized advantage for token t in the i -th output is defined as:

$$\hat{A}_{i,t} = \frac{R^{(i)} - \text{mean}(\{R^{(j)}\}_{j=1}^G)}{\text{std}(\{R^{(j)}\}_{j=1}^G)}. \quad (5)$$

The token-level importance weight is defined as:

$$r_{i,t}(\theta) = \frac{\pi_\theta(y_t^{(i)} | X, y_{<t}^{(i)})}{\pi_{\theta_{\text{ref}}}(y_t^{(i)} | X, y_{<t}^{(i)})}. \quad (6)$$

Then the GRPO objective with KL regularization and clipping is then given by:

$$\mathcal{J}_{\text{GRPO}}(\theta) = \mathbb{E}_{X \sim \mathcal{D}, \{Y^{(i)}\}_{i=1}^G \sim \pi_\theta(\cdot | X)} \left[\frac{1}{\sum_{i=1}^G \|Y^{(i)}\|} \sum_{i=1}^G \sum_{t=1}^{\|Y^{(i)}\|} \left(\min \left(r_{i,t}(\theta) \hat{A}_{i,t}, \text{clip}(r_{i,t}(\theta), 1 - \epsilon_{\text{low}}, 1 + \epsilon_{\text{high}}) \hat{A}_{i,t} \right) - \beta D_{\text{KL}}(\pi_\theta \| \pi_{\theta_{\text{ref}}}) \right) \right], \quad (7)$$

where $\|Y^{(i)}\|$ is the length of the sampled output, ϵ_{low} and ϵ_{high} are the clipping thresholds, and β controls the KL divergence penalty with respect to a reference policy $\pi_{\theta_{\text{ref}}}$. This objective encourages the model to improve outputs with relatively high rewards while staying close to the original behavior policy and preventing overfitting or reward hacking.

Besides, we also design different optimization strategies for the two tasks, including jointly optimizing both capabilities within a single model, as well as alternately optimizing the two capabilities in two adversarial models.

4 Experiments

4.1 Experimental Setup

Training Data We used the training set of T2I-CompBench [15] for the text-to-image generation part, which contains 5,600 text prompts. For the visual understanding part, we randomly sampled 2,800 images from the JourneyDB [37] and COCO118K [38] derived from COCO Caption [39] respectively. It is worth noting that the image and text training data are non-parallel, meaning that we did not use any annotated image-text pairs to train the model.

Baselines We employ the unified LMM Janus-Pro-7B [7] as our backbone, optimizing it with our dual self-reward mechanism in a self-supervised manner. We compare our tuned model with state-of-the-art (SOTA) models on visual understanding and generation tasks, including models that are designed only for understanding such as LLaVA [2] and InstructBLIP-7B [40], models designed only for generation tasks like CoMat [41] and LDM [14], as well as unified LMMs that can perform both tasks such as Chameleon [31] and Show-o [5]. All baselines can be found in Table 1, Table 2, and Table 3.

Evaluation Benchmarks We evaluate our method on visual understanding and generation benchmarks and follow their default settings. For visual generation, we use T2I-CompBench [15] and GenEval [16] as the evaluation benchmarks. We test on their original text prompts without any modification. T2I-CompBench comprises 6,000 compositional text prompts evaluating 3 categories (attribute binding, object relationships, and complex compositions) and 6 sub-categories (color binding, shape binding, texture binding, spatial relationships, non-spatial relationships, and complex compositions). GenEval [16] includes 6 tasks (single object, two objects, counting, colors, position, and color attributes). For visual understanding, we use HallusionBench (denoted as HalluBench) [42], LLaVABench, POPE [43], MMB [44], SEEDBench-IMG (denoted as SEED) [45], and MMMU [46].

Implementation Details We implement our method upon Trl³ code base and train with Deepspeed⁴. Zero-2. For each input, we sample 8 outputs for GRPO algorithm and select 2 of them for SimPO. The learning rate is set to 3e-6 with a cosine decay schedule, with a warmup of 5 steps. ϵ_{low} and ϵ_{high} are set to 0.2 and 0.28. β and γ in SimPO are set to 2.0 and 0.5, respectively. β in GRPO is set to 0.04. The batch size is set to 64, and the gradient_accumulation_step is set to 2, resulting in a global batch size of 128. The model is trained for 5 epochs on our training set.

4.2 Results on Visual Generation

We compare our model with the SOTA diffusion models and unified LMMs on the T2I-CompBench and GenEval benchmarks. The results are shown in Table 1 and Table 2, respectively. Our trained model is denoted as “Janus-Pro-7B + DSR”, where the model is optimized with DSR and SimPO in the unified strategy.

The results show that our model achieves substantial improvements over the baseline model, with an average increase of 11.68% on T2I-CompBench and overall 5% on GenEval. On T2I-CompBench, our model remarkably improves the performance in all categories, especially in attribute binding with an average improvement of 20%. In spatial relationships and complex compositions, our model also achieves impressive increases of 5% and 3%, respectively. Our model demonstrates the best performance in shape binding, texture binding, and complex compositions, and achieves the second best performance in color binding. On GenEval, our model improves over the baseline model, especially in counting and color attributes with an increase of 13% and 7%. It outperforms the diffusion models overall, achieving the best performance. These results demonstrate the effectiveness and superiority of our method in improving the text-to-image generation capabilities of LMMs, despite the fact that our model is optimized in a completely self-supervised manner without any external supervision or additional data.

Table 1: Evaluation on T2I-CompBench. Und. and Gen. denote “understanding” and “generation”, respectively. Higher (↑) values indicate better performance. The best score is in **bold**, with the second best score underlined. Line in blue is our model.

Model	Attribute Binding			Object Relationship		Complex↑
	Color↑	Shape↑	Texture↑	Spatial↑	Non-Spatial↑	
<i>Gen. Only</i>						
StrucDiffusion [47]	0.4990	0.4218	0.4900	0.1386	0.3111	0.3355
CompDiffusion [48]	0.4063	0.3299	0.3645	0.0800	0.2980	0.2898
Attend&Excite [49]	0.6400	0.4517	0.5963	0.1455	0.3109	0.3401
PixArt- α [50]	0.6690	0.4927	0.6477	0.2064	0.3197	0.3433
CoMat [41]	0.7827	0.5329	0.6468	0.2428	<u>0.3187</u>	0.3680
SD-v1.5 [14]	0.3758	0.3713	0.4186	0.1165	0.3112	0.3047
SD-XL-base-1.0 [51]	0.5879	0.4687	0.5299	0.2131	0.3119	0.3237
FLUX.1 [52]	0.7407	<u>0.5718</u>	0.6922	0.2863	0.3127	0.3703
<i>Und. and Gen.</i>						
Show-o [5]	0.56	0.41	0.46	0.20	0.30	0.29
Emu3 [4]	0.7544	0.5706	<u>0.7164</u>	–	–	–
Janus-Pro-7B [7]	0.6426	0.3487	0.4848	0.2061	0.3086	0.3510
Janus-Pro-7B + DSR	<u>0.7824</u> _{+14%}	0.5786 _{+23%}	0.7292 _{+24%}	<u>0.2524</u> _{+5%}	0.3141 _{+1%}	0.3858 _{+3%}

4.3 Results on Visual Understanding

For visual understanding, we test the models on the prevalent benchmarks, including HallusionBench (denoted as HalluBench) [42], LLaVABench, POPE [43], MMB [44], SEEDBench-IMG (denoted as SEED) [45], and MMMU [46], which are widely used to evaluate the understanding capabilities of LMMs. The experimental results can be found in Table 3.

³<https://github.com/huggingface/trl.git>

⁴<https://github.com/deepspeedai/DeepSpeed.git>

Table 2: Evaluation on GenEval.

Model	Single Obj.	Two Obj.	Counting	Colors	Position	Color Attri.	Overall↑
<i>Gen. Only</i>							
LlamaGen [3]	0.71	0.34	0.21	0.58	0.07	0.04	0.32
LDM [14]	0.92	0.29	0.23	0.70	0.02	0.05	0.37
SDv1.5 [14]	0.97	0.38	0.35	0.76	0.04	0.06	0.43
PixArt- α [50]	0.98	0.50	0.44	0.80	0.08	0.07	0.48
SDv2.1 [14]	0.98	0.51	0.44	0.85	0.07	0.17	0.50
DALL-E 2 [53]	0.94	0.66	0.49	0.77	0.10	0.19	0.52
Emu3-Gen [4]	0.98	0.71	0.34	0.81	0.17	0.21	0.54
SDXL [51]	0.98	0.74	0.39	0.85	0.15	0.23	0.55
DALL-E 3 [54]	0.96	0.87	0.47	0.83	0.43	0.45	0.67
SD3-Medium [55]	0.99	0.94	0.72	0.89	0.33	0.60	0.74
<i>Und. and Gen.</i>							
SEED-X [56]	0.97	0.58	0.26	0.80	0.19	0.14	0.49
Show-o [5]	0.95	0.52	0.49	0.82	0.11	0.28	0.53
D-DiT [57]	0.97	0.80	0.54	0.76	0.32	0.50	0.65
LWM [58]	0.93	0.41	0.46	0.79	0.09	0.15	0.47
Transfusion [59]	–	–	–	–	–	–	0.63
ILLUME [12]	0.99	0.86	0.45	0.71	0.39	0.28	0.61
TokenFlow-XL [58]	0.95	0.60	0.41	0.81	0.16	0.24	0.55
Chameleon [31]	–	–	–	–	–	–	0.39
Janus [6]	0.95	0.62	0.28	0.85	0.45	0.42	0.60
Janus-Pro-1B [7]	0.99	0.82	0.48	<u>0.90</u>	0.62	0.57	0.73
Janus-Pro-7B [7]	0.97	0.88	0.57	<u>0.90</u>	0.77	<u>0.64</u>	<u>0.79</u>
Janus-Pro-7B + DSR	0.99+2%	<u>0.89+1%</u>	<u>0.70+13%</u>	0.92+2%	0.82+5%	0.71+7%	0.84+5%

On HallusionBench and LLaVABench, our proposed method achieves substantial improvements over Janus-Pro-7B, the baseline model, with an increase of 1.9% and 7.5%, respectively. On other benchmarks, our model keeps the performance of Janus-Pro-7B, which is already a strong baseline. The results demonstrate that our method can improve the understanding capabilities of LMMs and maintain the original advanced performance, while remarkably improving the generation capabilities.

Table 3: Evaluation on understanding benchmarks.

Model	HallBench↑	LLaVA Bench↑	POPE↑	MMB↑	SEED↑	MMMU↑
<i>Und. Only</i>						
LLaVA [2]	21.6	57.2	76.3	38.7	33.5	34.1
LLaVA-v1.5 [60]	27.6	63.4	85.9	64.3	58.6	35.4
InstructBLIP-7B [40]	31.2	60.9	86.1	36.0	53.4	30.6
Emu3-Chat [4]	31.7	49.2	85.2	58.5	68.2	31.6
Qwen-VL-Chat [1]	36.8	67.7	74.9	60.6	58.2	37.0
Qwen2.5-VL-7B [61]	52.9	91.0	85.9	83.2	77.0	58.6
<i>Und. and Gen.</i>						
Chameleon-7B [31]	17.1	26.6	19.4	15.4	30.5	22.4
Show-o-256 [5]	–	–	73.8	–	–	25.1
Show-o-512 [5]	–	–	80.0	–	–	26.7
ILLUME [12]	–	–	88.5	65.1	72.9	38.2
TokenFlow-XL [58]	–	–	<u>86.8</u>	68.9	68.7	38.7
LWM [58]	–	–	75.2	–	–	–
VILA-U [30]	–	–	85.8	–	59.0	–
Janus-Pro-7B [7]	37.0	74.0	<u>86.8</u>	79.6	71.9	41.1
Janus-Pro-7B + DSR	<u>38.9</u>	<u>81.5</u>	86.6	<u>80.1</u>	71.9	<u>41.1</u>

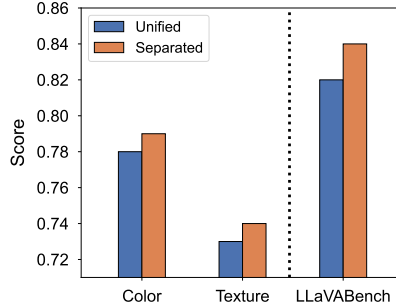


Figure 3: Comparison of optimization strategies.

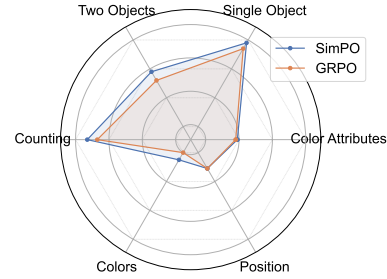


Figure 4: Comparison of optimization methods.

4.4 Ablation Study

We conduct ablation studies to investigate the effectiveness of the proposed unified optimization strategy on the two capabilities and the effectiveness of the dual self-reward. We compare the performance of the following setups: 1) the baseline model (Janus-Pro-7B) without any optimization; 2) only optimizing the generation capability; 3) only optimizing the understanding capability; 4) jointly optimizing the two capabilities. These setups are evaluated on the T2I-CompBench, HalluBench, and LLaVABench benchmarks. The default optimization method is SimPO [35]. The results are shown in Table 4.

Table 4: Ablation study of unified optimization manner on T2I-CompBench, HalluBench, and LLaVABench.

Model	Training	T2I CompBench			HalluBench \uparrow	LLaVABench \uparrow
		Color \uparrow	Shape \uparrow	Texture \uparrow		
Janus-Pro-7B	–	0.6426	0.3487	0.4848	37.0	74.0
	Only Und.	0.5313	0.3355	0.4138	38.9	81.4
	Only Gen.	0.7824	0.5786	0.7272	37.3	77.3
	Und. + Gen.	0.7773	0.5763	0.7292	38.9	81.5

The results show that optimizing only the generation capability significantly improves performance on the T2I-CompBench benchmark, while this setup offers limited gains on the HalluBench and LLaVABench benchmarks. Conversely, optimizing only the understanding capability yields improvements on HalluBench and LLaVABench but slightly degrades generation performance. The unified optimization approach—jointly optimizing both capabilities—achieves a balanced and substantial improvement across all benchmarks. These results demonstrate the effectiveness of the proposed unified optimization strategy in enhancing both generation and understanding capabilities without compromising one for the other.

Moreover, the capability optimized during training shows corresponding improvements, which indicates that our proposed dual self-reward mechanism is effective.

4.5 Investigation of Different Optimization Strategies

We have demonstrated that the proposed dual self-reward mechanism and the unified optimization strategy are effective in jointly improving the generation and understanding capabilities in the previous sections. To further stimulate the potential of the proposed approach, we explore a different optimization strategy by training two separate models for the two capabilities and optimizing them alternately. Specifically, we train one generation model and one understanding model in an adversarial manner, where each model is trained based on the other one’s dual rewards. At each epoch, we freeze one model and update the other one, and vice versa.

The results are shown in Figure 3. We call these two models ‘separate models’ and the model trained with the unified optimization strategy ‘unified model’. It can be observed that the performance of the

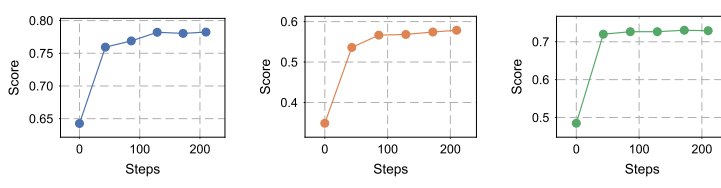


Figure 5: Evolution on T2I-CompBench during training.

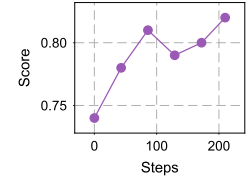


Figure 6: Evolution on LLaVABench during training.

separate models is better than the unified model on each type of task. This indicates that the better understanding model provides better dual rewards for the generation model, and vice versa. By this the two models can be trained in an adversarial-like manner, where one focuses on generation and the other on understanding, to mutually enhance their performance with better reward signals.

In addition, we also compare two different optimization methods, including the SimPO [35] and GRPO [33] in our framework on T2I-CompBench. The results can be seen in Figure 3, which shows that SimPO is slightly better than GRPO. This is likely because DSR contains a certain level of noise, while SimPO selects only the samples with the highest and lowest rewards, naturally serving as a denoising process.

4.6 Evolution of Capabilities with Training

We test the intermediate checkpoints to investigate the evolution of the capabilities of the model during training. We conduct this experiment on T2I-CompBench and LLaVABench. The results are shown in Figure 5 and Figure 6.

We can observe that the generation capability improves steadily over the training process, while the understanding capability improves at the beginning and stabilizes earlier. This indicates that the understanding of the baseline model is already strong and thus is easy to converge, while the generation capability can be improved further.

5 Conclusion

In this work, we proposed a dual self-reward mechanism to enhance the generation and understanding capabilities of LMMs in an efficient, self-supervised, and unified manner. By leveraging the dual self-reward mechanism, we designed a unified optimization strategy that jointly optimizes the two capabilities of the unified LMM, leading to substantial improvements in both generation and understanding tasks. We also investigated the performance of different optimization strategies, including the joint optimization strategy with a unified model and the adversarial-like optimization strategy with two separate models. Extensive experiments on various visual understanding and generation benchmarks demonstrate the effectiveness of our proposed method. Overall, our method showcases the potential of improving the generation and understanding capabilities of LMMs in a self-supervised and unified manner, paving the way for future research on multimodal alignment.

Limitations Despite the promising results achieved by our dual self-reward mechanism in visual understanding and generation tasks, how to effectively extend this approach to other modalities like audio remains to be explored. Additionally, the dual self-reward mechanism requires the backbone LMM to have undergone basic semantic alignment. How to integrate our approach into the pre-training process of multimodal large models presents a promising direction for future research.

References

[1] Jinze Bai, Shuai Bai, Shusheng Yang, Shijie Wang, Sinan Tan, Peng Wang, Junyang Lin, Chang Zhou, and Jingren Zhou. Qwen-vl: A frontier large vision-language model with versatile abilities. *arXiv preprint arXiv:2308.12966*, 1(2):3, 2023.

[2] Haotian Liu, Chunyuan Li, Qingyang Wu, and Yong Jae Lee. Visual instruction tuning. *Advances in neural information processing systems*, 36:34892–34916, 2023.

[3] Peize Sun, Yi Jiang, Shoufa Chen, Shilong Zhang, Bingyue Peng, Ping Luo, and Zehuan Yuan. Autoregressive model beats diffusion: Llama for scalable image generation. *arXiv preprint arXiv:2406.06525*, 2024.

[4] Xinlong Wang, Xiaosong Zhang, Zhengxiong Luo, Quan Sun, Yufeng Cui, Jinsheng Wang, Fan Zhang, Yueze Wang, Zhen Li, Qiying Yu, et al. Emu3: Next-token prediction is all you need. *arXiv preprint arXiv:2409.18869*, 2024.

[5] Jinheng Xie, Weijia Mao, Zechen Bai, David Junhao Zhang, Weihao Wang, Kevin Qinghong Lin, Yuchao Gu, Zhijie Chen, Zhenheng Yang, and Mike Zheng Shou. Show-o: One single transformer to unify multimodal understanding and generation. *arXiv preprint arXiv:2408.12528*, 2024.

[6] Chengyue Wu, Xiaokang Chen, Zhiyu Wu, Yiyang Ma, Xingchao Liu, Zizheng Pan, Wen Liu, Zhenda Xie, Xingkai Yu, Chong Ruan, et al. Janus: Decoupling visual encoding for unified multimodal understanding and generation. *arXiv preprint arXiv:2410.13848*, 2024.

[7] Xiaokang Chen, Zhiyu Wu, Xingchao Liu, Zizheng Pan, Wen Liu, Zhenda Xie, Xingkai Yu, and Chong Ruan. Janus-pro: Unified multimodal understanding and generation with data and model scaling. *arXiv preprint arXiv:2501.17811*, 2025.

[8] Jiaming Ji, Jiayi Zhou, Hantao Lou, Boyuan Chen, Donghai Hong, Xuyao Wang, Wenqi Chen, Kaile Wang, Rui Pan, Jiahao Li, Mohan Wang, Josef Dai, Tianyi Qiu, Hua Xu, Dong Li, Weipeng Chen, Jun Song, Bo Zheng, and Yaodong Yang. Align anything: Training all-modality models to follow instructions with language feedback, 2024. URL <https://arxiv.org/abs/2412.15838>.

[9] Yassine Ouali, Adrian Bulat, Brais Martinez, and Georgios Tzimiropoulos. Clip-dpo: Vision-language models as a source of preference for fixing hallucinations in llms. In *European Conference on Computer Vision*, pages 395–413. Springer, 2024.

[10] Dongzhi Jiang, Ziyu Guo, Renrui Zhang, Zhuofan Zong, Hao Li, Le Zhuo, Shilin Yan, Pheng-Ann Heng, and Hongsheng Li. T2i-r1: Reinforcing image generation with collaborative semantic-level and token-level cot, 2025. URL <https://arxiv.org/abs/2505.00703>.

[11] Leigang Qu, Haochuan Li, Wenjie Wang, Xiang Liu, Juncheng Li, Liqiang Nie, and Tat-Seng Chua. Silmm: Self-improving large multimodal models for compositional text-to-image generation, 2025. URL <https://arxiv.org/abs/2412.05818>.

[12] Chunwei Wang, Guansong Lu, Junwei Yang, Runhui Huang, Jianhua Han, Lu Hou, Wei Zhang, and Hang Xu. Illume: Illuminating your llms to see, draw, and self-enhance. *arXiv preprint arXiv:2412.06673*, 2024.

[13] Ce Zhang, Zifu Wan, Zhehan Kan, Martin Q. Ma, Simon Stepputtis, Deva Ramanan, Russ Salakhutdinov, Louis-Philippe Morency, Katia P. Sycara, and Yaqi Xie. Self-correcting decoding with generative feedback for mitigating hallucinations in large vision-language models. In *The Thirteenth International Conference on Learning Representations*, 2025.

[14] Robin Rombach, Andreas Blattmann, Dominik Lorenz, Patrick Esser, and Björn Ommer. High-resolution image synthesis with latent diffusion models. In *2022 IEEE/CVF Conference on Computer Vision and Pattern Recognition (CVPR)*, pages 10674–10685. IEEE, 2022.

[15] Kaiyi Huang, Kaiyue Sun, Enze Xie, Zhenguo Li, and Xihui Liu. T2i-compbench: a comprehensive benchmark for open-world compositional text-to-image generation. In *Proceedings of the 37th International Conference on Neural Information Processing Systems*, pages 78723–78747, 2023.

[16] Dhruba Ghosh, Hannaneh Hajishirzi, and Ludwig Schmidt. Geneval: an object-focused framework for evaluating text-to-image alignment. In *Proceedings of the 37th International Conference on Neural Information Processing Systems*, pages 52132–52152, 2023.

[17] OpenAI. Gpt-4v(ision) system card. 2023. URL https://cdn.openai.com/papers/GPTV_System_Card.pdf.

[18] Anthropic. Introducing the next generation of claudie. 2024. URL <https://www.anthropic.com/news/claudie-3-family>.

[19] Deyao Zhu, Jun Chen, Xiaoqian Shen, Xiang Li, and Mohamed Elhoseiny. Minigpt-4: Enhancing vision-language understanding with advanced large language models. In *12th International Conference on Learning Representations, ICLR 2024*, 2024.

[20] Zhe Chen, Jiannan Wu, Wenhai Wang, Weijie Su, Guo Chen, Sen Xing, Muyan Zhong, Qinglong Zhang, Xizhou Zhu, Lewei Lu, et al. Intern vl: Scaling up vision foundation models and aligning for generic visual-linguistic tasks. In *2024 IEEE/CVF Conference on Computer Vision and Pattern Recognition (CVPR)*, pages 24185–24198. IEEE, 2024.

[21] Haoyu Lu, Wen Liu, Bo Zhang, Bingxuan Wang, Kai Dong, Bo Liu, Jingxiang Sun, Tongzheng Ren, Zhusu Li, Hao Yang, et al. Deepseek-vl: towards real-world vision-language understanding. *arXiv preprint arXiv:2403.05525*, 2024.

[22] Zhiyu Wu, Xiaokang Chen, Zizheng Pan, Xingchao Liu, Wen Liu, Damai Dai, Huazuo Gao, Yiyang Ma, Chengyue Wu, Bingxuan Wang, et al. Deepseek-vl2: Mixture-of-experts vision-language models for advanced multimodal understanding. *arXiv preprint arXiv:2412.10302*, 2024.

[23] Aaron van den Oord, Oriol Vinyals, and Koray Kavukcuoglu. Neural discrete representation learning. In *Proceedings of the 31st International Conference on Neural Information Processing Systems*, pages 6309–6318, 2017.

[24] Patrick Esser, Robin Rombach, and Bjorn Ommer. Taming transformers for high-resolution image synthesis. In *2021 IEEE/CVF Conference on Computer Vision and Pattern Recognition (CVPR)*, pages 12868–12878. IEEE, 2021.

[25] Quan Sun, Qiying Yu, Yufeng Cui, Fan Zhang, Xiaosong Zhang, Yueze Wang, Hongcheng Gao, Jingjing Liu, Tiejun Huang, and Xinlong Wang. Emu: Generative pretraining in multimodality. In *The Twelfth International Conference on Learning Representations*, 2024.

[26] Quan Sun, Yufeng Cui, Xiaosong Zhang, Fan Zhang, Qiying Yu, Yueze Wang, Yongming Rao, Jingjing Liu, Tiejun Huang, and Xinlong Wang. Generative multimodal models are in-context learners. In *Proceedings of the IEEE/CVF Conference on Computer Vision and Pattern Recognition*, pages 14398–14409, 2024.

[27] Hanrong Ye, De-An Huang, Yao Lu, Zhiding Yu, Wei Ping, Andrew Tao, Jan Kautz, Song Han, Dan Xu, Pavlo Molchanov, et al. X-vila: Cross-modality alignment for large language model. *arXiv preprint arXiv:2405.19335*, 2024.

[28] Shengqiong Wu, Hao Fei, Leigang Qu, Wei Ji, and Tat-Seng Chua. Next-gpt: Any-to-any multimodal llm. In *Forty-first International Conference on Machine Learning*, 2024.

[29] Jun Zhan, Junqi Dai, Jiasheng Ye, Yunhua Zhou, Dong Zhang, Zhigeng Liu, Xin Zhang, Ruibin Yuan, Ge Zhang, Linyang Li, et al. Anygpt: Unified multimodal llm with discrete sequence modeling. In *Proceedings of the 62nd Annual Meeting of the Association for Computational Linguistics (Volume 1: Long Papers)*, pages 9637–9662, 2024.

[30] Yecheng Wu, Zhuoyang Zhang, Junyu Chen, Haotian Tang, Dacheng Li, Yunhao Fang, Ligeng Zhu, Enze Xie, Hongxu Yin, Li Yi, et al. Vila-u: a unified foundation model integrating visual understanding and generation. *arXiv preprint arXiv:2409.04429*, 2024.

[31] Pan Lu, Baolin Peng, Hao Cheng, Michel Galley, Kai-Wei Chang, Ying Nian Wu, Song-Chun Zhu, and Jianfeng Gao. Chameleon: Plug-and-play compositional reasoning with large language models. *Advances in Neural Information Processing Systems*, 36:43447–43478, 2023.

[32] Rafael Rafailev, Archit Sharma, Eric Mitchell, Christopher D Manning, Stefano Ermon, and Chelsea Finn. Direct preference optimization: Your language model is secretly a reward model. *Advances in Neural Information Processing Systems*, 36:53728–53741, 2023.

[33] Zhihong Shao, Peiyi Wang, Qihao Zhu, Runxin Xu, Junxiao Song, Xiao Bi, Haowei Zhang, Mingchuan Zhang, YK Li, Y Wu, et al. Deepseekmath: Pushing the limits of mathematical reasoning in open language models. *arXiv preprint arXiv:2402.03300*, 2024.

[34] Wei Shen, Rui Zheng, Wenyu Zhan, Jun Zhao, Shihan Dou, Tao Gui, Qi Zhang, and Xuan-Jing Huang. Loose lips sink ships: Mitigating length bias in reinforcement learning from human feedback. In *Findings of the Association for Computational Linguistics: EMNLP 2023*, pages 2859–2873, 2023.

[35] Yu Meng, Mengzhou Xia, and Danqi Chen. Simpo: Simple preference optimization with a reference-free reward. *Advances in Neural Information Processing Systems*, 37:124198–124235, 2024.

[36] Qiying Yu, Zheng Zhang, Ruofei Zhu, Yufeng Yuan, Xiaochen Zuo, Yu Yue, Weinan Dai, Tiantian Fan, Gaohong Liu, Lingjun Liu, Xin Liu, Haibin Lin, Zhiqi Lin, Bole Ma, Guangming Sheng, Yuxuan Tong, Chi Zhang, Mofan Zhang, Wang Zhang, Hang Zhu, Jinhua Zhu, Jiaze Chen, Jiangjie Chen, Chengyi Wang, Hongli Yu, Yuxuan Song, Xiangpeng Wei, Hao Zhou, Jingjing Liu, Wei-Ying Ma, Ya-Qin Zhang, Lin Yan, Mu Qiao, Yonghui Wu, and Mingxuan Wang. Dapo: An open-source llm reinforcement learning system at scale, 2025. URL <https://arxiv.org/abs/2503.14476>.

[37] Keqiang Sun, Junting Pan, Yuying Ge, Hao Li, Haodong Duan, Xiaoshi Wu, Renrui Zhang, Aojun Zhou, Zipeng Qin, Yi Wang, et al. Journeydb: a benchmark for generative image understanding. In *Proceedings of the 37th International Conference on Neural Information Processing Systems*, pages 49659–49678, 2023.

[38] Bo Li, Yuanhan Zhang, Dong Guo, Renrui Zhang, Feng Li, Hao Zhang, Kaichen Zhang, Peiyuan Zhang, Yanwei Li, Ziwei Liu, et al. Llava-onevision: Easy visual task transfer. *arXiv preprint arXiv:2408.03326*, 2024.

[39] Tsung-Yi Lin, Michael Maire, Serge Belongie, James Hays, Pietro Perona, Deva Ramanan, Piotr Dollár, and C Lawrence Zitnick. Microsoft coco: Common objects in context. In *Computer vision–ECCV 2014: 13th European conference, zurich, Switzerland, September 6–12, 2014, proceedings, part v 13*, pages 740–755. Springer, 2014.

[40] Wenliang Dai, Junnan Li, DONGXU LI, Anthony Tiong, Junqi Zhao, Weisheng Wang, Boyang Li, Pascale N Fung, and Steven Hoi. Instructblip: Towards general-purpose vision-language models with instruction tuning. *Advances in Neural Information Processing Systems*, 36:49250–49267, 2023.

[41] Dongzhi Jiang, Guanglu Song, Xiaoshi Wu, Renrui Zhang, Dazhong Shen, Zhuofan Zong, Yu Liu, and Hongsheng Li. Comat: Aligning text-to-image diffusion model with image-to-text concept matching. *Advances in Neural Information Processing Systems*, 37:76177–76209, 2024.

[42] Zhiyuan Zhao, Bin Wang, Linke Ouyang, Xiaoyi Dong, Jiaqi Wang, and Conghui He. Beyond hallucinations: Enhancing lvlms through hallucination-aware direct preference optimization. *arXiv preprint arXiv:2311.16839*, 2023.

[43] Yifan Li, Yifan Du, Kun Zhou, Jinpeng Wang, Wayne Xin Zhao, and Ji-Rong Wen. Evaluating object hallucination in large vision-language models. In *Proceedings of the 2023 Conference on Empirical Methods in Natural Language Processing*, pages 292–305, 2023.

[44] Yuan Liu, Haodong Duan, Yuanhan Zhang, Bo Li, Songyang Zhang, Wangbo Zhao, Yike Yuan, Jiaqi Wang, Conghui He, Ziwei Liu, et al. Mmbench: Is your multi-modal model an all-around player? In *European Conference on Computer Vision*, pages 216–233, 2024.

[45] Bohao Li, Yuying Ge, Yixiao Ge, Guangzhi Wang, Rui Wang, Ruimao Zhang, and Ying Shan. Seed-bench: Benchmarking multimodal large language models. In *Proceedings of the IEEE/CVF Conference on Computer Vision and Pattern Recognition*, pages 13299–13308, 2024.

[46] Xiang Yue, Yuansheng Ni, Kai Zhang, Tianyu Zheng, Ruoqi Liu, Ge Zhang, Samuel Stevens, Dongfu Jiang, Weiming Ren, Yuxuan Sun, et al. Mmmu: A massive multi-discipline multimodal understanding and reasoning benchmark for expert agi. In *Proceedings of the IEEE/CVF Conference on Computer Vision and Pattern Recognition*, pages 9556–9567, 2024.

[47] Weixi Feng, Xuehai He, Tsu-Jui Fu, Varun Jampani, Arjun Akula, Pradyumna Narayana, Sugato Basu, Xin Eric Wang, and William Yang Wang. Training-free structured diffusion guidance for compositional text-to-image synthesis. *arXiv preprint arXiv:2212.05032*, 2022.

[48] Nan Liu, Shuang Li, Yilun Du, Antonio Torralba, and Joshua B Tenenbaum. Compositional visual generation with composable diffusion models. In *European Conference on Computer Vision*, pages 423–439. Springer, 2022.

[49] Hila Chefer, Yuval Alaluf, Yael Vinker, Lior Wolf, and Daniel Cohen-Or. Attend-and-excite: Attention-based semantic guidance for text-to-image diffusion models. *ACM Transactions on Graphics (TOG)*, 42(4):1–10, 2023.

[50] Junsong Chen, YU Jincheng, GE Chongjian, Lewei Yao, Enze Xie, Zhongdao Wang, James Kwok, Ping Luo, Huchuan Lu, and Zhenguo Li. Pixart-alpha: Fast training of diffusion transformer for photorealistic text-to-image synthesis. In *The Twelfth International Conference on Learning Representations*, 2024.

[51] Dustin Podell, Zion English, Kyle Lacey, Andreas Blattmann, Tim Dockhorn, Jonas Müller, Joe Penna, and Robin Rombach. Sdxl: Improving latent diffusion models for high-resolution image synthesis. *arXiv preprint arXiv:2307.01952*, 2023.

[52] Black Forest Labs. Flux. <https://github.com/black-forest-labs/flux>, 2024.

[53] Aditya Ramesh, Prafulla Dhariwal, Alex Nichol, Casey Chu, and Mark Chen. Hierarchical text-conditional image generation with clip latents. *arXiv preprint arXiv:2204.06125*, 2022.

[54] James Betker, Gabriel Goh, Li Jing, Tim Brooks, Jianfeng Wang, Linjie Li, Long Ouyang, Juntang Zhuang, Joyce Lee, Yufei Guo, et al. Improving image generation with better captions. *Computer Science*. <https://cdn.openai.com/papers/dall-e-3.pdf>, 2(3):8, 2023.

[55] Patrick Esser, Sumith Kulal, Andreas Blattmann, Rahim Entezari, Jonas Müller, Harry Saini, Yam Levi, Dominik Lorenz, Axel Sauer, Frederic Boesel, et al. Scaling rectified flow transformers for high-resolution image synthesis. In *International Conference on Machine Learning*, pages 12606–12633. PMLR, 2024.

[56] Yuying Ge, Sijie Zhao, Jinguo Zhu, Yixiao Ge, Kun Yi, Lin Song, Chen Li, Xiaohan Ding, and Ying Shan. Seed-x: Multimodal models with unified multi-granularity comprehension and generation. *arXiv preprint arXiv:2404.14396*, 2024.

[57] Zijie Li, Henry Li, Yichun Shi, Amir Barati Farimani, Yuval Kluger, Linjie Yang, and Peng Wang. Dual diffusion for unified image generation and understanding. *arXiv preprint arXiv:2501.00289*, 2024.

[58] Hao Liu, Wilson Yan, Matei Zaharia, and Pieter Abbeel. World model on million-length video and language with ringattention. *arXiv e-prints*, pages arXiv–2402, 2024.

[59] Chunting Zhou, Lili Yu, Arun Babu, Kushal Tirumala, Michihiro Yasunaga, Leonid Shamis, Jacob Kahn, Xuezhe Ma, Luke Zettlemoyer, and Omer Levy. Transfusion: Predict the next token and diffuse images with one multi-modal model. *arXiv preprint arXiv:2408.11039*, 2024.

[60] Haotian Liu, Chunyuan Li, Yuheng Li, and Yong Jae Lee. Improved baselines with visual instruction tuning. In *Proceedings of the IEEE/CVF Conference on Computer Vision and Pattern Recognition*, pages 26296–26306, 2024.

[61] Shuai Bai, Keqin Chen, Xuejing Liu, Jialin Wang, Wenbin Ge, Sibo Song, Kai Dang, Peng Wang, Shijie Wang, Jun Tang, et al. Qwen2. 5-vl technical report. *arXiv preprint arXiv:2502.13923*, 2025.

- [62] Siyan Zhao, Devaansh Gupta, Qingqing Zheng, and Aditya Grover. d1: Scaling reasoning in diffusion large language models via reinforcement learning, 2025. URL <https://arxiv.org/abs/2504.12216>.
- [63] Alec Radford, Jong Wook Kim, Chris Hallacy, Aditya Ramesh, Gabriel Goh, Sandhini Agarwal, Girish Sastry, Amanda Askell, Pamela Mishkin, Jack Clark, Gretchen Krueger, and Ilya Sutskever. Learning transferable visual models from natural language supervision. In Marina Meila and Tong Zhang, editors, *Proceedings of the 38th International Conference on Machine Learning*, volume 139 of *Proceedings of Machine Learning Research*, pages 8748–8763. PMLR, 18–24 Jul 2021. URL <https://proceedings.mlr.press/v139/radford21a.html>.
- [64] Junke Wang, Zhi Tian, Xun Wang, Xinyu Zhang, Weilin Huang, Zuxuan Wu, and Yu-Gang Jiang. SimpleAR: Pushing the frontier of autoregressive visual generation through pretraining, sft, and rl, 2025. URL <https://arxiv.org/abs/2504.11455>.

A Technical Appendices

A.1 Qualitative Comparison

We present qualitative comparisons of Janus-Pro-7B and Janus-Pro-7B tuned with DSR on visual generation and understanding tasks in Figure 7 and Figure 8, respectively. The images and responses are sampled from the models with the same setup, where the temperature is set to 1.0 and the random seed is set to 42.

As illustrated in Figure 7, the images generated by Janus-Pro-7B with DSR are distinctly more aligned with the text prompts compared to those generated by the baseline Janus-Pro-7B. The images exhibit improved detail, quality, and alignment with the prompts, demonstrating the effectiveness of DSR in enhancing visual generation capabilities. In Figure 8, we observe that responses of Janus-Pro-7B with DSR are more accurate for the given image and question, compared to those of Janus-Pro-7B. This indicates that the understanding capabilities of the model are also improved with DSR.

Both figures highlight the substantial improvements in both visual generation and understanding tasks achieved by the proposed DSR when applied to the unified LMM.

A.2 Demonstration of DSR

We present demonstrations of our dual self-reward mechanism with Janus-Pro-7B, which can be found in Figure 9 and Figure 10.

A.3 Experiments with Show-o

We conduct additional experiments with another backbone, Show-o [5], to further validate the effectiveness of our method.

Show-o is a unified multimodal model that unifies autoregressive and discrete diffusion modeling for inputs and outputs in different modalities. It applies full attention for image tokens and causal attention for text tokens, and it is trained with a combination of next token prediction (NTP) and mask token prediction (MTP) objectives. To ensure efficiency, we follow *difffu*-GRPO [62], using one-step unmasking with randomly dropped input text tokens condition to obtain the estimated log-probability of the generated image tokens.

The results are shown in table 5.

The results show that our method can also improve the performance of Show-o, gaining more than 5% on average on T2I-CompBench. This demonstrates the general applicability of our proposed DSR.

A.4 Experiments using CLIP as Reward Model

We conduct additional experiments using CLIP [63] as the reward model, following SimpleAR [64]. We only optimize the visual generation capability of Janus-Pro-7B with SimPO, and the results are shown in Table 6 and Table 7.

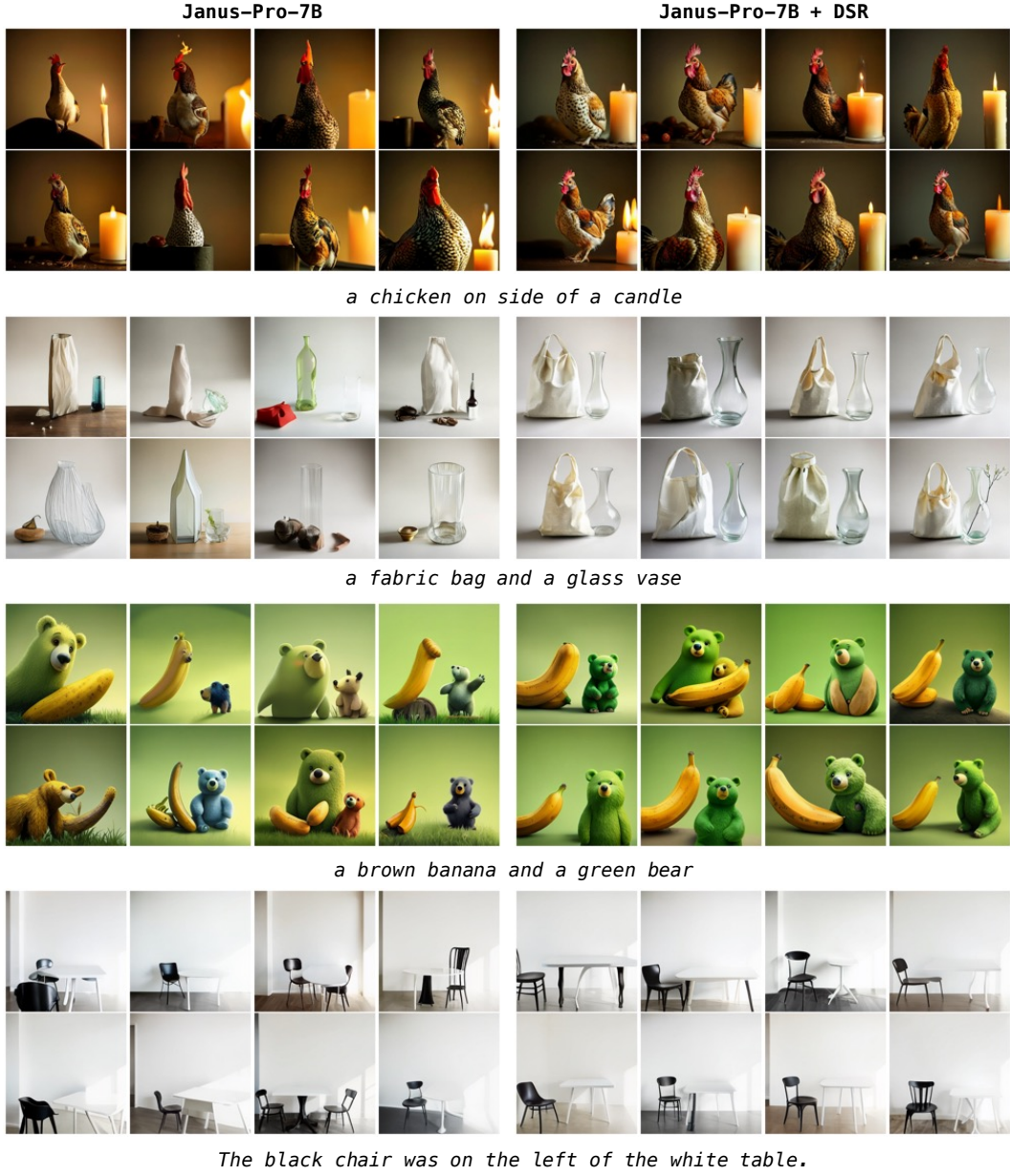


Figure 7: Qualitative comparison of visual generation. We sample multiple images for same text prompts using Janus-Pro-7B and reinforced Janus-Pro-7B with the proposed DSR.

When using CLIP as the reward model and optimizing only the visual generation capability, the performance of the model on the T2I-CompBench is improved substantially, which is slightly worse than the model optimized with our DSR. But for the understanding, the performance with CLIP is not improved or even slightly decreased, which is remarkably worse than ours. This indicates that: 1) our DSR is more effective than CLIP; 2) only optimizing the visual generation capability may hurt the understanding capability of the model, while our unified DSR can improve both the understanding and generation capabilities of the model.

A.5 Details of the Understanding Benchmarks

We provide the details of the understanding benchmarks used in our experiments in this section.

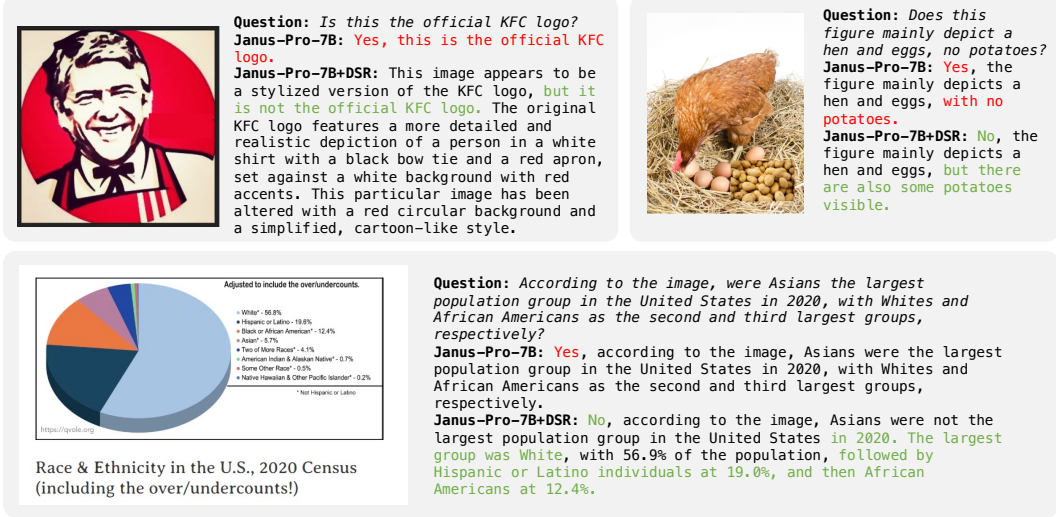


Figure 8: Qualitative comparison of visual understanding. We sample multiple responses for same image with a question using Janus-Pro-7B and reinforced Janus-Pro-7B with the proposed DSR.



Figure 9: Demonstration of our dual self-reward for visual generation. We sample multiple images for a given text prompt and then compute DSR for the images. In this demonstration, the first generated image is the best one, which is also the one with the highest DSR.

HalluBench [42] is a benchmark to evaluate hallucination of VLMs. It asks a set of visual questions with one original image and one modified image (the answers for a question can be different, considering the image content).

LLaVABench evaluates model capabilities on challenging tasks and novel domains through a diverse set of 24 images and 60 questions, covering indoor/outdoor scenes, memes, paintings, sketches, etc., each paired with detailed, manually curated descriptions and carefully selected questions.

POPE [43] is a benchmark for object hallucination evaluation. It contains approximately 8910 cases over three tracks of object hallucination: random, popular, and adversarial. We report the overall results on the random track, following the previous works.

MMB [44] is a multi-modality benchmark that performs objective evaluation for VLMs with over 3,000 multiple-choice questions covering 20 ability dimensions.

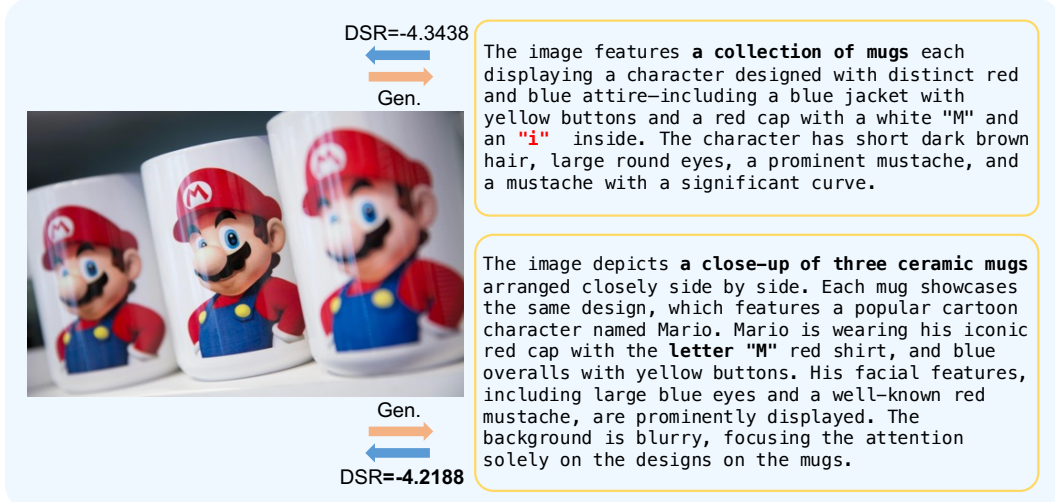


Figure 10: Demonstration of our dual self-reward for visual understanding. We sample multiple text descriptions for a given image and then compute DSR for the descriptions. In this demonstration, the upper generated description is better, which is also the one with the higher DSR.

Table 5: Evaluation on T2I-CompBench. Und. and Gen. denote “understanding” and “generation”. Higher (\uparrow) values indicate better performance. The best score is in **bold**, with the second best score underlined. Line in blue is our tuned model. The line with \dagger is the results we reproduce for fair comparison.

Model	Attribute Binding			Object Relationship		Complex \uparrow
	Color \uparrow	Shape \uparrow	Texture \uparrow	Spatial \uparrow	Non-Spatial \uparrow	
<i>Gen. Only</i>						
StrucDiffusion [47]	0.4990	0.4218	0.4900	0.1386	0.3111	0.3355
CompDiffusion [48]	0.4063	0.3299	0.3645	0.0800	0.2980	0.2898
Attend&Excite [49]	0.6400	0.4517	0.5963	0.1455	0.3109	0.3401
PixArt- α [50]	0.6690	0.4927	0.6477	0.2064	0.3197	0.3433
CoMat [41]	0.7827	0.5329	0.6468	0.2428	<u>0.3187</u>	0.3680
SD-v1.5 [14]	0.3758	0.3713	0.4186	0.1165	0.3112	0.3047
SD-XL-base-1.0 [51]	0.5879	0.4687	0.5299	0.2131	0.3119	0.3237
FLUX.1 [52]	0.7407	<u>0.5718</u>	0.6922	0.2863	0.3127	<u>0.3703</u>
<i>Und. and Gen.</i>						
Emu3 [4]	0.7544	0.5706	<u>0.7164</u>	—	—	—
Janus-Pro-7B \dagger [7]	0.6426	0.3487	0.4848	0.2061	0.3086	0.3510
Janus-Pro-7B + DSR	<u>0.7824+14%</u>	0.5786+23%	0.7292+24%	<u>0.2524+5%</u>	<u>0.3141+1%</u>	0.3858+3%
Show-o [5]	0.56	0.41	0.46	0.20	0.30	0.29
Show-o \dagger [5]	0.5892	0.4002	0.4489	0.2268	0.3026	0.3058
Show-o + DSR	<u>0.6894+10%</u>	<u>0.4953+10%</u>	<u>0.5530+10%</u>	0.2253	0.3015	<u>0.3268+2%</u>

SEED [45] consists of 24K multiple-choice questions with accurate human annotations, which cover 27 evaluation dimensions.

MMMU [46] includes multi-choice questions and open-ended QA, with 62 and 988 cases, respectively.

Table 6: Evaluation on T2I-CompBench. Und. and Gen. denote “understanding” and “generation”, respectively. Higher (\uparrow) values indicate better performance. Line in blue is our tuned model. The line with \dagger is the results reproduced by us for fair comparison.

Model	Attribute Binding			Object Relationship		Complex \uparrow
	Color \uparrow	Shape \uparrow	Texture \uparrow	Spatial \uparrow	Non-Spatial \uparrow	
Janus-Pro-7B \dagger [7]	0.6426	0.3487	0.4848	0.2061	0.3086	0.3510
Janus-Pro-7B + CLIP	0.7700	0.5609	0.7320	0.2302	0.3144	0.3863
Janus-Pro-7B + DSR	0.7824+14%	0.5786+23%	0.7292+24%	0.2524+5%	0.3141+1%	0.3858+3%

Table 7: Evaluation on understanding benchmarks.

Model	HallBench \uparrow	LLaVABench \uparrow	POPE \uparrow	MMB \uparrow	SEED \uparrow	MMMU \uparrow
Janus-Pro-7B \dagger [7]	37.0	74.0	86.8	79.6	71.9	41.1
Janus-Pro-7B + CLIP	36.9	74.0	86.6	79.6	71.9	41.3
Janus-Pro-7B + DSR	38.9	81.5	86.6	80.1	71.9	41.1

B Broader Impacts

Positive Impacts Our method contributes to improving the semantic consistency and alignment of LMMs, particularly in challenging compositional scenarios. This advancement could benefit a wide range of applications. For instance, better text-to-image alignment enables more accurate and reliable visual content generation in design, communication, and accessibility tools for visually impaired users. Similarly, improved multimodal understanding helps build safer and more context-aware assistant systems, such as educational tutoring agents or medical image interpreters, where understanding and describing visual inputs accurately is critical.

Potential Negative Impacts Enhanced text-to-image generation capabilities may be misused to produce highly convincing fake content, contributing to misinformation, deepfakes, or non-consensual imagery.

Safeguards This paper does not release any new datasets. All experiments are conducted using publicly available LMMs, datasets, and benchmarks. Future releases based on our work will incorporate appropriate usage guidelines, safety filters for generated content, and bias auditing mechanisms.